Published in final edited form as:
Neuroimage. 2010 February 1; 49(3): 2083. doi:10.1016/j.neuroimage.2009.10.035.

Multiple Indicators of Age-related Differences in Cerebral White Matter and the Modifying Effects of Hypertension

S. Burgmans[a,b], **M.P.J. van Boxtel**[a,b], **E.H.B.M. Gronenschild**[a,b], **E.F.P.M. Vuurman**[b,c], **P. Hofman**[a,b,d], **H.B.M. Uylings**[a,b,e], **J. Jolles**[a,b,f], and **N. Raz**[g,h]

[a]Department of Psychiatry and Neuropsychology, School for Mental Health and Neuroscience, Maastricht University, Maastricht, the Netherlands [b]European Graduate School of Neuroscience (EURON), Maastricht University, Maastricht, the Netherlands [c]Department of Neuropsychology and Psychopharmacology, Faculty of Psychology and Neuroscience, Maastricht University, Maastricht, the Netherlands [d]Department of Radiology, University Hospital Maastricht, Maastricht, the Netherlands [e]Department of Anatomy and Neuroscience, VU University Medical Center, Amsterdam, the Netherlands [f]AZIRE Research Institute, Faculty of Psychology and Education, VU University, Amsterdam, the Netherlands [g]Institute of Gerontology, Wayne State University, Detroit, MI, United States

Abstract

We investigated differences associated with age and hypertension, a common risk factor for vascular disease, in three aspects of white matter integrity – gross regional volumes of the white matter, volume of the white matter hyperintensities (WMH) and diffusion properties. We acquired MRI scans on 93 adult volunteers (age 50-77 years; 36 with diagnosis of hypertension or elevated blood pressure), and obtained all measures in seven brain regions: frontal, temporal, parietal and occipital white matter, and the genu, body and splenium of the corpus callosum. The results demonstrated robust age-related differences in diffusion-based indices of cerebral white matter integrity and age-related increase in the WMH volume, but no age differences in the gross regional volumes of the white matter. Hypertension was associated with decline in fractional anisotropy, and exacerbated age differences in fractional anisotropy more than those in the volume of WMH. These findings indicate that of all examined measures, diffusion-based indices of white matter integrity may be the most sensitive indicators of global and regional declines and vascular damage in the aging brain.

Introduction

Advanced age is associated with substantial alterations of the cerebral white matter (Kemper, 1994; Kennedy & Raz, 2009a), and age-related deterioration of the white matter integrity has been linked to declines in processing speed, memory, and executive functioning (Bucur et al., 2007; Burns et al., 2005; Gunning-Dixon & Raz, 2000; Raz et al., 2007; Sullivan & Pfefferbaum, 2006; Verdelho et al., 2007). There are multiple ways to assess white matter integrity *in vivo*, including macroscopic indices, such as the gross volume or the burden of

hCorresponding author: Naftali Raz, Institute of Gerontology, Wayne State University, 87 East Ferry St., Detroit, MI 48202, United States, nraz@wayne.edu, fax +1-508-256-55689.

white matter hyperintensities (WMH), and measures of microintegrity derived from examination of diffusion properties of the white matter.

Each of the described indices is characterized by a different shape of relationship to calendar age. White matter volume is smaller in children than in young adults (Lenroot & Giedd, 2006) but larger in middle-aged adults than in older persons (Bartzokis et al., 2004), with the prefrontal regions showing greater age-related shrinkage, especially under the influence of vascular risk factors (Raz & Rodrigue, 2006). White matter hyperintensities, which appear as bright regions on T2-weighted MRI scans, represent multiple types of vascular and cellular pathology, including arteriosclerotic and ischemic lesions, patches of demyelination, axonal loss, gliosis and expansion of perivascular spaces (De Leeuw et al., 2001; Pantoni & Garcia, 1997). Although present throughout the cerebral white matter, and increasingly so with age (De Leeuw et al., 2001; Kennedy & Raz, 2009a), WMH may be more frequent and voluminous in the frontal lobe than elsewhere in the brain (Fazekas et al., 2005; Raz et al., 2003; Raz et al., 2007; Tullberg et al., 2004; Yoshita et al., 2006). Parietal and occipital WMH, which are relatively rare in healthy adults, may proliferate with increase in cardiovascular risk (Artero et al., 2004; Raz et al., 2007; Yoshita et al., 2006).

Diffusion-tensor imaging (DTI) yields multiple indices of white matter microintegrity: apparent diffusion coefficient (ADC), fractional anisotropy (FA), mean diffusivity (MD), axial diffusivity (λ_{ax}), and radial diffusivity (λ_{rad}). Decrease of FA with a concomitant increase in MD is interpreted as demyelination and axonal loss, whereas a decrease of FA without MD change is presumed to reflect Wallerian degeneration. In addition, reduced radial diffusivity has been primarily associated with demyelination, whereas increased axial diffusivity is viewed as a reflection of axonal damage (Song et al., 2003; Song et al., 2005; Sun et al., 2006; Y. Zhang et al., 2008). It is worth noting, however, that recent reports advise caution in interpreting variations in radial and axial diffusivity (Wheeler-Kingshott & Cercignani, 2009).

The extant literature on age-related differences in diffusion properties of the cerebral white matter suggests that advanced age is associated with reduced anisotropy (lower FA) and increased diffusivity in many white matter regions (Bhagat & Beaulieu, 2004; Chun et al., 2000; Deary et al., 2006; Furutani et al., 2005; Grieve et al., 2007; L. Huang et al., 2006; Pfefferbaum et al., 2005; Pfefferbaum & Sullivan, 2003; Pfefferbaum et al., 2000; Salat, Tuch, Greve et al., 2005; Salat, Tuch, Hevelone et al., 2005; Sullivan et al., 2001; Y. T. Zhang et al., 2005). Although variability in region selection hampers comparison of DTI-based findings across studies, a relatively consistent finding is that the anterior regions of the brain, especially the genu of the corpus callosum, exhibit stronger negative age differences than in the posterior regions, such as the splenium (Abe et al., 2002; Ardekani et al., 2007; Bhagat & Beaulieu, 2004; Chepuri et al., 2002; Grieve et al., 2007; Head et al., 2004; Hugenschmidt et al., 2008; Kochunov et al., 2007; Madden et al., 2007; O'Sullivan et al., 2001; Ota et al., 2006; Pfefferbaum et al., 2005; Pfefferbaum et al., 2000; Salat, Tuch, Hevelone et al., 2005; Sullivan et al., 2001).

Although numerous studies that focus on age differences in each index of white matter integrity, only few examine the relationship among multiple measures. Two reports suggested that DTI may be the most sensitive imaging measure of age-related white matter damage (Hugenschmidt et al., 2008; Schiavone et al., 2009). However, another investigation found that age-related decline of diffusion-based indices was primarily explained by white matter atrophy and white matter lesion formation. That study concluded that age-related loss of white matter integrity is not part of the physiological aging process *per se* (Vernooij et al., 2008). Nonetheless, in a second study on the same sample (Vernooij et al., 2009), the authors concluded that in investigating the relation between white matter integrity and cognition, diffusion-based measures might have an added value beyond macroscopical indices, such as regional volume

and WMH. The implication is that differences in DTI-derived indices may reflect pathophysiological processes that differ from those expressed in white matter atrophy and WMH proliferation. Thus, the issue of relative importance of different indices of white matter integrity in detecting age differences remains unresolved and calls for a direct comparison of the abovementioned measures within a single sample.

Integrity of the cerebral white matter is negatively affected not only by age but also by vascular risk factors, such as hypertension (De Leeuw et al., 2001; Kennedy & Raz, 2009a; Pantoni & Garcia, 1997; Raz, 2000), the prevalence of which increases with age (Franklin et al., 1997). In comparison to their normotensive peers, persons with hypertension evidence smaller prefrontal volumes and faster shrinkage of the prefrontal white matter (Raz et al., 2005; Raz et al., 2003), larger WMH burden (Goldstein et al., 2005; Henskens et al., 2009; Raz et al., 2007; Skoog, 1998; Van Boxtel et al., 2006), and lower anisotropy of white matter diffusion (L. Huang et al., 2006; Kennedy & Raz, 2009b). Thus, hypertension exacerbates age differences in white matter integrity, but it is unclear which, if any of those indices is the best in detecting the effects of vascular risk on the aging brain.

Because diffusion-based indices of white matter integrity reflect microstructural properties, whereas gross volume and WMH show the relatively global and cumulative effects of multiple influences, we hypothesized that DTI-derived measures would show the greatest age- and hypertension-related difference in the white matter. To test this hypothesis, we compared within a single sample three types of measures: regional white matter volumes, WMH, and four indices based on water diffusion in the white matter (fractional anisotropy, mean diffusivity, axial and radial diffusivity). This comparison, to the best of our knowledge, has never been done in studies of hypertension as a modifier of brain aging.

Materials and Methods

Participants

The participants for this study were selected from the first wave of a longitudinal MRI study of 219 healthy community volunteers (aged 18-81 years) from the Metro Detroit area, who were recruited through advertisements in the local media and screened via a telephone interview and health questionnaire. The reasons for exclusion from the study were a history of cardiovascular, neurological and psychiatric conditions, head trauma with a loss of consciousness for more than 5 minutes, history of alcohol and drug abuse, or a diagnosis of diabetes or thyroid disorder. The items used to screen for cardiovascular disease included an open question on any kind of diseases or complaints related to the heart or the large blood vessels as well as taking specific medications prescribed for treatment of cardiovascular conditions. The participants had corrected visual acuity of 20/50 or better (Optic 2000, Stereo Optic) and adequate hearing acuity (hearing threshold levels 40 dB or better for frequencies of 500-4000 Hz; Maico, MA27). To screen for dementia and depression we used the MMSE (Folstein et al., 1975) and the Center for Epidemiologic Studies Depression Scale (CES-D; Weissman et al., 1977). Only persons who scored 26 or higher on MMSE and 15 or below on CES-D were invited to participate. All participants provided written informed consent in accord with university and hospital review board guidelines.

For the present study that was focused on phenomena (e.g. WMH) that are rarely observed in younger adults, we selected 93 participants of fifty years of age and older (range: 50-77 years). Thirty-six participants were hypertensive. Thirty-one of these participants reported a history of hypertension diagnosed by their physician and were all taking at least one antihypertensive medication; the mean duration of treatment was 6.7 years. Five additional participants who were not diagnosed with hypertension were classified as hypertensive because they had an abnormal high average systolic blood pressure at the research center (> 140 mmHg; averaged

across at least three measurements), or an abnormal high average diastolic blood pressure (> 90 mmHg). The remaining 57 participants were normotensive based on all available criteria. Healthy participants did not differ from the hypertensive group in age, sex, education and ethnicity (see Table 1).

Blood pressure measurement

To measure blood pressure we used a random zero mercury sphygmomanometer (BMS 12-S25) with a standard blood pressure cuff (Omron Professional). All measures were performed on the left arm with participants seated and the forearm positioned on the table. Trained laboratory technicians conducted the measurements. Blood pressure measures were obtained on three to four different occasions and averages of available measurements were used in the present study.

Image acquisition

Four series of MRI images were acquired on a 4T MRI system (Bruker Biospin, Ettlingen, Germany) with an 8-channel RF coil. Magnetization-prepared rapid gradient echo (MPRAGE) T1-weighted images were acquired in the coronal plane with the following parameters: TR = 1600 ms, TE = 4.38 ms, TI = 800 ms, FOV = 256 × 256 mm^2, in plane resolution = 0.67 × 0.67 mm^2, slice thickness = 1.34 mm, matrix size = 384 × 384, number of slices = 176. Fluid-attenuated inversion recovery (FLAIR) images were acquired in the axial (horizontal) plane, with TR = 8440 ms, TE = 112 ms, TI = 2200 ms, FA = 150°, FOV = 256 × 256 mm^2, contiguous slice thickness = 2 mm, matrix size = 256 × 256. A Turbo Spin-Echo (TSE) sequence was used to acquire 50 contiguous axial slices of Proton-density (PD)/T2-weighted images with TR = 3700 ms, TE = 19 ms/96 ms, FA = 150°, FOV = 256 × 256 mm^2, slice thickness = 2 mm, matrix size = 256 × 256. Diffusion Weighted Images (DTI) were acquired with the parameters TR = 4900 ms, TE = 79 ms, 6 diffusion directions, 10 averages, 41 slices, FOV = 256 × 256 mm^2, voxel size = 2 × 2 × 3 mm^3, GeneRalized Autocalibrating Partially Parallel Acquisitions (GRAPPA) acceleration factor 2. The MR images used in this study were free of pathological findings.

Image analyses

Before processing, we used the MNI software (Montreal Neurological Institute, Montreal, USA) to correct the T1-weighted and FLAIR images for magnetic field inhomogeneities (Sled et al., 1998). All analyses were performed in native space, with an exception for the T1-weighted images. The latter were transformed into standardized MNI space (see Figure 1) via a linear transformation, which allowed transfer of the images and templates back into the native space (see Collins et al., 1994 for the linear transformation procedure). The DTI images were processed with the BrainVoyagerQX software, version 1.10 (Brain Innovation, Maastricht, the Netherlands) in native space.

For several post-processing steps (except for the DTI analysis) we used the custom software package GIANT, developed at the Maastricht School for Mental Health and Neuroscience (EHBMG). First, regions of interest (ROIs) were traced on the T1-weighted image of each participant. The second step consisted of three different image analyses: volumetric measures on the T1-weighted images, WMH measurements on the FLAIR images, and diffusion indices analysis on the DTI. At the third step, six outcome measurements were calculated within each ROI: volume of the white matter ROIs, volume of the WMH, and DTI-derived indices: mean FA, mean MD, mean λ_{ax} and mean λ_{rad}. Figure 1 provides a brief overview of all post-processing steps.

Region of Interest analysis (Figure 1, first row)—First, all T1-weighted images were transformed into standardized MNI space via a linear transformation, and an average brain was

created out of 10 randomly selected brains. Second, an operator (SB) manually drew the contours of five regions of interest (ROIs) on the average brain, thus creating an average ROI template. Third, this average ROI template was mapped on the brains of all participants. As the ROI borders of this average template did not match completely the ROI borders of the individual brains, all borders were edited manually to ensure neuroanatomical correctness of the ROI demarcation. GIANT displayed the T1-weighted images in a triplanar view, together with a 3D rotatable outer surface display, which facilitated accurate identification of the sulci. The editing was performed on coronal, axial and sagittal slices, depending on the ROI, which took about four hours per brain. This process generated 93 individual ROI templates. Fourth, the individual ROI templates were transferred from standardized MNI space back into native space.

Demarcation of the ROIs (Figure 2)

Corpus Callosum—The corpus callosum was traced on 20 sagittal slices: 10 per hemisphere, starting from the midsagittal slice. In each slice, the corpus callosum was divided into genu, body, and splenium according to a procedure depicted in Figure 2 and based on the method described by Hofer and Frahm (Hofer & Frahm, 2006) and the callosal radiation map created by Huang and colleagues (H. Huang et al., 2005).

Frontal lobe—The posterior border was defined by the central sulcus and the ventral border by the lateral sulcus. In the white matter, a straight horizontal line was drawn on the axial plane (i.e. perpendicular to the longitudinal fissure) between the medial part of the central sulcus and the longitudinal fissure.

Parietal Lobe—The anterior border was defined by the central sulcus and the ventral border by the corpus callosum, lateral ventricles, basal ganglia and lateral sulcus. The posterior border was defined medially by the parieto-occipital sulcus and laterally by several sulci (e.g. the anterior occipital sulcus) that connect the parieto-occipital sulcus with the pre-occipital notch.

Occipital Lobe—The anterior border was medially defined by the parieto-occipital sulcus and ventrally by the pre-occipital notch. Laterally, the anterior border was defined by several sulci that connect the parieto-occipital sulcus with the pre-occipital notch.

Temporal Lobe—The dorsal border was defined by the lateral sulcus and the posterior border by the occipital lobe.

The hemispheres were separated within each ROI (except for the corpus callosum) by a straight vertical line on the coronal plane. The outer surface of the ROIs was defined by the outer surface of the brain. For this purpose we used the FSL Brain Extraction Tool (Smith, 2002) which generated the inner-cranium contours. These contours were also used to calculate the intracranial volume (ICV) for each participant.

Volumetric image analysis (Figure 1, second row)—The individual ROI templates were overlaid on the T1-weighted images in standardized MNI space. To segment the T1-weighted images into gray matter, white matter and cerebro-spinal fluid, we used the MNI software (Zijdenbos et al., 2002). All voxels that were recognized as white matter were selected within each ROI, which resulted in a segmented ROI template. Finally, the segmented ROI template was transformed back into native space. The ROIs were verified slice-by-slice, and all instances of suboptimal segmentation were corrected manually. Finally, the volumes of each white matter ROI were calculated. To test the reliability of this method, the operator (SB) performed the whole procedure twice on ten randomly selected brains. This procedure yielded

high test-retest reliability for each ROI, with an intraclass correlation coefficients > 0.90 (ICC, formula 1,1: one-way random effects, Shrout & Fleiss, 1979).

White Matter Hyperintensities (Figure 1, third row)—To quantify the volumes of WMH on the FLAIR images we used a semi-automatic tool (GIANT). First, the algorithm was trained to classify WMH correctly. For this purpose, the image intensity scale of the FLAIR images was standardized (Nyúl & Udupa, 1999). Next, five FLAIR scans with a substantial amount of white matter lesions were selected and the white matter lesions in these stacks were traced manually. These manual tracings were used to derive parameters for the automatic classification of the WMH. Second, the actual quantification of WMH was performed semi-automatically. Axial FLAIR and T2-weighted images were displayed and aligned side by side on the computer monitor. This allowed visual inspection of the scan and easy identification of WMH. In each slice, a WMH was indicated manually by clicking in its region, thus generating a seed point and providing starting parameters for region growing. Manual corrections were performed when necessary. Finally, the total volume of the WMH within each ROI was calculated. The WMH quantification was performed twice on ten randomly selected brains by the same rater (SB), and yielded high test-retest reliability: intraclass correlation coefficient = 0.99 (ICC 1,1, Shrout & Fleiss, 1979).

Diffusion Tensor Imaging (Figure 1, fourth row)—FA maps were generated from the DTI images by BrainVoyagerQX. The images were inspected for relevant motion artifacts, but none were found. Since DTI is very sensitive to data transformation, we minimized manipulations of the original scan data, and performed the analyses in the native space. Each DTI scan was aligned to the T1-image in native space and an FA map was calculated without applying smoothing filters. The mean FA values of the individual brains in native space were used for the statistical analyses. To isolate the white matter and to exclude the gray matter and CSF voxels, we applied a threshold of FA < 0.20. The accuracy of this white matter FA map was verified by visual inspection after overlaying the FA map on the T1-weighted image and evaluating its match to the white matter. Finally, the individual ROI template was overlayed on the FA map and the mean FA of each ROI was calculated. The same procedure was followed for the Mean Diffusivity (MD), Axial Diffusivity (λ_{ax}) and Radial Diffusivity (λ_{rad}) maps, except for the threshold (i.e., no additional threshold was applied to those maps).

Because representation of biophysical properties of the tissue by diffusion tensor eigenvalues may depend on the orientation of the principal eigenvector (Madden et al., 2009), we computed relative axial and radial diffusivity indices from the eigenvalues (λ_1, λ_2 and λ_3) of the estimated diffusion tensors. Relative Axial diffusivity (AX) was calculated by the formula $AX = (\lambda_1 - \lambda_2)/\lambda_1$, creating a dimensionless index that was high for linear or prolate tensor shapes and representing diffusivity parallel to the primary fiber orientation. Relative radial diffusivity (RAD) was calculated by the formula $RAD = (\lambda_2 - \lambda_3)/\lambda_1$, as a dimensionless index with high values for planar or oblate tensor shapes reflecting diffusivity in the direction perpendicular to the white matter tract (Roebroeck et al., 2008; Westin et al., 2002).

Statistical analyses

For statistical analyses, we used the Statistical Package for Social Sciences (SPSS Inc, Chicago), version 15.0 for Windows. First, the descriptive statistics for the two groups were calculated. The effects of sex and hypertension on the continuous variables were assessed with univariate ANOVA under the General Linear Model (GLM) procedure. Group differences of the categorical variables were assessed with the χ^2 test. Second, effects of age and hypertension were tested using multivariate ANOVA from the General Linear Model (GLM) menu. Six separate multivariate analyses were performed to evaluate age and hypertension effects in each ROI. Each multivariate analysis contained a different white matter indicator as the dependent

variable in the GLM model: white matter volumes, white matter hyperintensities, FA values, MD values, AX values and RAD values. Sex was included as a categorical predictor in all analyses. White matter volumes were corrected for intracranial volume by including intracranial volume as covariate. To minimize collinearity, age and intracranial volume were centered at their sample means, thus setting the means of centered variables at 0. The age effects of WMH were assessed on the log- transformed WMH volumes because of leftward skew in the raw data. The statistical significance of all interactions involving the repeated measure (ROI) was corrected for violation of sphericity assumption via the Huynh-Feldt correction factor. The data were checked for normality, homogeneity of variances, and influential outliers. Finally, non-linear (quadratic) effects were investigated by including centered terms for age and age^2 within the same GLM.

Results

Sample characteristics

Table 1 displays the sample characteristics and the effects of hypertension and sex thereon. As expected, the blood pressure was significantly higher in the hypertensive participants compared to their normotensive counterparts, and most of the hypertensives used anti-hypertensive medication. The two groups did not differ with respect to age, education, ethnic composition, MMSE and intracranial volume. There were neither sex differences, nor sex × hypertension interactions for any of the descriptors, except for intracranial volume, which was larger in men.

Associations between age and white matter measures

Table 2 and Figure 3 show the associations between age and white matter measures in the normotensive and hypertensive participants. Although there was a substantial effect of age on white matter integrity, the magnitude of that effect differed among the three types of indicators: volumes, hyperintensities and diffusion-based measure (see below). Whereas age effects on the WMH and DTI measures were robust and widespread, there were hardly any significant age differences in white matter volumes. We found no significant quadratic age effects. The variance of age did not differ between the hypertensive and normotensive participants: Levene's test for equality of variances: $F = 0.41$, $p = 0.520$.

Modifying influence of hypertension on white matter measures

The analyses presented in Tables 2A and 2B revealed significant effects of hypertension on the white matter volumes, WMH and FA. In addition, the observed significant hypertension × age interaction effects on the WMH, FA and (to a smaller extent) relative radial diffusivity suggested a modifying influence of hypertension. The magnitude of the age × hypertension interaction effect differed among the four indices of white matter integrity. For FA, the incremental addition of explained variance, ΔR^2 (R^2 of the full model minus R^2 of the model without interaction term), was 3.7%. In comparison, ΔR^2 was only 0.3% for the total white matter volume, 0.2% for the total WMH volume, and 0.3% for the total brain MD, with none significantly different from zero.

Although the ROI × age × hypertension interaction was not significant, the effect of hypertension appeared the strongest for the frontal lobe FA (effect of hypertension: $F = 13.16$, $p < 0.001$; age × hypertension interaction: $F = 13.92$, $p < 0.001$, $\Delta R^2 = 9.4\%$). As illustrated in Figure 3, age-related differences (the slopes of regression estimating the rate of decline in FA as a function of increasing age) were greater for hypertensive than for normotensive participants. For hypertensives, the slope was $b = -0.00089$, 95% Confidence Interval CI [-0.00122; -0.00055], $\beta = -0.69$, $p < 0.001$; for normotensives, the slope was $b = -0.00039$, 95% CI [-0.00068; 0.00010], $\beta = -0.34$, $p = 0.010$. No significant interaction effects on the white matter volumes, MD and relative axial diffusivity were observed.

When regional FA measures were adjusted for the corresponding regional WMH and white matter volumes via covariance analysis, most of the age effects and age × hypertension interactions remained significant. After introduction of WMH and white matter volume as covariates, only two age effects on FA were no longer significant: for the genu ($F = 2.25$, $p = 0.138$) and body ($F = 1.12$, $p = 0.292$) of the corpus callosum. In addition, the age × hypertension interaction for the parietal lobe FA was rendered nonsignificant as well ($F = 1.14$, $p = 0.289$).

Associations among the indices of white matter integrity

The association among the four main indices of white matter integrity (volumes, hyperintensities, FA and MD) appear in Table 3. In summary, the FA measures correlated with nearly all MD measures, indicating that these two DTI indices were mutually dependent. However, most other correlations between the four indices were not significant, and the significant correlations were mostly small. Thus, as a rule, volumes, hyperintensities, and diffusion-based indices (FA and MD) were mutually independent or weakly associated at best. With regard to the four DTI outcome measures, we observed a decrease of the FA and an increase of the MD with advanced age. In addition, we found a slightly greater age-related decrease of axial diffusivity than radial diffusivity in all brain areas. The slope of the regression on age was steeper in axial diffusivity (β for total = -0.60) than in radial diffusivity (β for total = -0.50). A test for the equality of two dependent correlations demonstrated that the difference between the two slopes was significant: $t = 16.05$, $df = 90$, $p < 0.001$ (Williams, 1959).

Regional differences in white matter deterioration

The regional differences depended upon the selection of white matter integrity measure and on the presence of hypertension. Notably, there were no substantial differences between the left and right hemisphere (results not shown). The effect of hypertension seems to be the largest in the FA measure of the frontal lobe (effect of hypertension: $F = 13.16$, $p < 0.001$; age × hypertension interaction: $F = 13.92$, $p < 0.001$, $\Delta R^2 = 9.4\%$). In addition, age effects on the corpus callosum FA were significantly stronger in the genu ($b = -0.00375$, 95%CI [-0.00584; -0.00167], $\beta = -0.36$; $p = 0.001$) and body ($b = -0.00152$, 95%CI [-0.00232; -0.00072], $\beta = -0.37$; $p < 0.001$) than in the splenium ($b = -0.00051$, 95%CI [-.00146; 0.00044], $\beta = -0.11$; $p = 0.286$) as indicated by a significant ROI × age interaction in the full sample: $F(1.20) = 6.89$, $p = 0.007$.

Discussion

The main finding in the present study is that in detecting age-related deterioration of white matter, diffusion-based directional index of white matter integrity, FA, may be more sensitive than other measures, such as WMH burden and regional volume. Mean diffusivity increased with age, indicating general reduction in barriers to diffusion, regardless of direction. However, age-related differences in relative axial diffusivity exceeded those in relative radial diffusivity, although both significantly decreased with age. Thus, age-related deterioration of the white matter may be more likely to stem from axonal damage than from demyelination. The latter inference, however, has to be taken with caution, as the recent studies question the interpretation of radial and axial diffusivity parameters in the cerebral white matter (Wheeler-Kingshott & Cercignani, 2009). In addition to its stronger association with age, FA, in comparison to other indices of white matter integrity, also showed a greater modifying influence of hypertension on age-related differences, whereas MD evidenced no differences associated with hypertension. In contrast to FA, hypertensive participants showed increased WMH volume only in the parietal lobes, thus replicating previously reported pattern of increased posterior WMH burden in hypertension (Artero et al., 2004; Raz et al., 2007).

Most of the present findings are in accord with the extant findings of age-related variability in the cerebral white matter integrity, including the regional pattern of the differences (Abe et al., 2002; Burns et al., 2005; Goldstein et al., 2005; L. Huang et al., 2006; Raz et al., 2007; Salat, Tuch, Greve et al., 2005; Salat, Tuch, Hevelone et al., 2005; Van Boxtel et al., 2006). First, in agreement with a recent report (Vernooij et al., 2008), we observed no substantial differences between the left and right hemisphere. Second, in agreement with numerous reports (see Kennedy & Raz, 2009a and Madden et al., 2009 for reviews), we found significantly greater age differences in the DTI indices for the genu of the corpus callosum in comparison to the splenium.

With regard to the etiology of white matter pathology, our comparison between the four DTI parameters suggests that white matter decline in normal brain aging reflects axonal loss and, to a lesser degree, demyelination. This contradicts several previous reports that found age-related differences primarily in radial diffusivity, and inferred that demyelination, and not axonal damage dominate the aging of the cerebral white matter (Bhagat & Beaulieu, 2004; Madden et al., 2009; Y. Zhang et al., 2008). However, in accord with our findings, several recent studies reported age-related differences in both axial and radial diffusivity (Sullivan et al., 2008; Vernooij et al., 2008; Zahr et al., 2009), thus indicating the presence of axonal changes along with alterations in the myelin sheath (Paus, 2009). A recent review of the extant DTI studies revealed a complex pattern of age differences in radial and axial diffusivity with some regions exhibiting age-related differences in axial, others in radial, and yet others – in both diffusivity indices (see Madden et al., 2009).

A possible explanation of such inter-study variability is that diffusivity changes represent a dynamic process that may vary across region, subject and time intervals. Thus, the etiology behind age-related differences in diffusion-based indices of white matte integrity remains to be elucidated. Moreover, it is unlikely that DTI-based measures of axial and radial diffusivity are specific enough to distinguish axon- and myelin-related processes (Paus, 2009; Wheeler-Kingshott & Cercignani, 2009), and we must interpret the neurobiological implications of DTI findings with due caution.

We found no substantial age differences in the white matter volume. The literature on that topic is inconsistent (see Raz, 2005 for a review). White matter volume exhibits highly nonlinear trajectories of aging and development (Bartzokis et al., 2004; Lenroot & Giedd, 2006). Moreover, in cross-sectional studies, such as the present one, some regions may show smaller effects or greater individual differences confounded with age (e.g., Raz et al., 2005). Thus, the likelihood of finding age differences in white matter volume may depend on multiple factors: the age range of the sample, the precision of regional demarcation, and presence of vascular risk. As we observed, nonetheless, age differences with WMH and DTI-based measures, it is plausible that in the middle-age and late adulthood, volumetric white matter measures are less sensitive to mild white matter deterioration than are WMH and DTI indices. An intriguing question of whether white matter shrinkage and formation of WMH lesions precede or follow microstructural deterioration can be answered only in a longitudinal study.

The anisotropic structure of the white matter is not preserved in the WMH (Vernooij et al., 2009), and one would expect that heavier WMH burden would be associated with lower FA. However, our findings do not support the conclusion that nearly all age differences in regional white matter integrity can be explained by white matter atrophy and white matter lesions (Vernooij et al., 2008), and our results are in accord with a recent report of only partial association between WMH and FA (Kennedy & Raz, 2009b). Although the extent of WMH burden accounted for some of the age differences in FA, most of age differences in FA were still significant after correction for WMH and white matter volume. Notably, in some regions, such as the corpus callosum, substantial age differences in FA were observed in the absence

of local WMH, but were attenuated by accounting for WMH in the hemispheric regions presumably connected by the relevant callosal fibers. In general, the associations between FA and WMH or volume were weak or nonsignificant. We can speculate that diffusion-based indices of white matter integrity reflect earlier or more subtle age-related changes than coarser measures such as WMH and volumes do. Alternately, deterioration of the hemispheric white matter (WMH) may cause changes in microintegrity of the connecting white matter (corpus callosum).

Interpretations of the findings presented here are bound by several limitations. First, although DTI-based indices, such as FA are useful indicators of white matter integrity, one should bear in mind that they might reflect particular structural properties of intact white matter in regions with high variation in directionality, i.e. multiple crossing and “kissing” fibres (Madden et al., 2009). Second, the sample size could be too small to reveal subtle but significant age differences in the white matter volumes. Third, age-related differences in white matter volume may be limited to specific locales, and the analytic methods employed in this study were too coarse to detect such associations. Finally, the cross-sectional design precludes assessment of actual age changes or causality. Therefore, we could not, for instance, evaluate the temporal order of white matter shrinkage, formation of WMH lesions, and microstructural deterioration.

In conclusion, the results of this study suggest that DTI-based indices of white matter integrity are more sensitive for detecting age-related vulnerability and the modifying influence of vascular risk on brain aging than measures of white matter volume and WMH burden. Thus, assessment of regional diffusion properties is a good candidate for an outcome measure in evaluation of interventions aimed at alleviating age-related declines.

Acknowledgments

We thank Kristen Kennedy, Karen Rodrigue, Cheryl Dahle, Andrew Bender, Awantika Deshmukh, Yiqin Yang, and Peng Yuan, Wayne State University (Detroit, MI), for preparation of the MRI images and Pim Pullens, Maastricht University (Netherlands), for his help in DTI analyses. We also thank Claude Lepage (MNI) for his assistance in the use of the MNI software. The study was supported by a National Institutes of Health grant R37 AG-011230 to NR.

References

Abe O, Aoki S, Hayashi N, Yamada H, Kunimatsu A, Mori H, et al. Normal aging in the central nervous system: Quantitative MR diffusion-tensor analysis. Neurobiol Aging 2002;23(3):433–441. [PubMed: 11959406]

Ardekani S, Kumar A, Bartzokis G, Sinha U. Exploratory voxel-based analysis of diffusion indices and hemispheric asymmetry in normal aging. Magn Reson Imaging 2007;25(2):154–167. [PubMed: 17275609]

Artero S, Tiemeier H, Prins ND, Sabatier R, Breteler MM, Ritchie K. Neuroanatomical localisation and clinical correlates of white matter lesions in the elderly. J Neurol Neurosurg Psychiatry 2004;75(9): 1304–1308. [PubMed: 15314121]

Bartzokis G, Lu PH, Mintz J. Quantifying age-related myelin breakdown with MRI: Novel therapeutic targets for preventing cognitive decline and Alzheimer's disease. J Alzheimers Dis 2004;6(6 Suppl):S53–59. [PubMed: 15665415]

Bhagat YA, Beaulieu C. Diffusion anisotropy in subcortical white matter and cortical gray matter: changes with aging and the role of CSF-suppression. J Magn Reson Imaging 2004;20(2):216–227. [PubMed: 15269946]

Bucur B, Madden DJ, Spaniol J, Provenzale JM, Cabeza R, White LE, et al. Age-related slowing of memory retrieval: Contributions of perceptual speed and cerebral white matter integrity. Neurobiol Aging 2007;29(7):1070–1079. [PubMed: 17383774]

Burns JM, Church JA, Johnson DK, Xiong C, Marcus D, Fotenos AF, et al. White matter lesions are prevalent but differentially related with cognition in aging and early Alzheimer disease. Arch Neurol 2005;62(12):1870–1876. [PubMed: 16344345]

Chepuri NB, Yen YF, Burdette JH, Li H, Moody DM, Maldjian JA. Diffusion anisotropy in the corpus callosum. Am J Neuroradiol 2002;23(5):803–808. [PubMed: 12006281]

Chun T, Filippi CG, Zimmerman RD, Ulug AM. Diffusion changes in the aging human brain. Am J Neuroradiol 2000;21(6):1078–1083. [PubMed: 10871018]

Collins DL, Neelin P, Peters TM, Evans AC. Automatic 3D intersubject registration of MR volumetric data in standardized Talairach space. J Comput Assist Tomogr 1994;18(2):192–205. [PubMed: 8126267]

De Leeuw, FE.; De Groot, JC.; Breteler, MMB. White matter changes: Frequency and risk factors. In: Pantoni, L.; Inzitari, D.; W, A., editors. The Matter of White Matter: Clinical and Pathophysiological Aspects of White Matter Disease Related to Cognitive Decline and Vascular Dementia. Academic Pharmaceutical Productions; Utrecht: 2001. p. 19-33.

Deary IJ, Bastin ME, Pattie A, Clayden JD, Whalley LJ, Starr JM, et al. White matter integrity and cognition in childhood and old age. Neurology 2006;66(4):505–512. [PubMed: 16505302]

Fazekas F, Ropele S, Enzinger C, Gorani F, Seewann A, Petrovic K, et al. MTI of white matter hyperintensities. Brain 2005;128(Pt 12):2926–2932. [PubMed: 15958507]

Folstein MF, Folstein SE, McHugh PR. “Mini-mental state”. A practical method for grading the cognitive state of patients for the clinician. J Psychiatr Res 1975;12(3):189–198. [PubMed: 1202204]

Franklin SS, Gustin Wt, Wong ND, Larson MG, Weber MA, Kannel WB, et al. Hemodynamic patterns of age-related changes in blood pressure. The Framingham Heart Study. Circulation 1997;96(1):308–315. [PubMed: 9236450]

Furutani K, Harada M, Minato M, Morita N, Nishitani H. Regional changes of fractional anisotropy with normal aging using statistical parametric mapping (SPM). J Med Invest 2005;52(34):186–190. [PubMed: 16167537]

Goldstein IB, Bartzokis G, Guthrie D, Shapiro D. Ambulatory blood pressure and the brain: a 5-year follow-up. Neurology 2005;64(11):1846–1852. [PubMed: 15955932]

Grieve SM, Williams LM, Paul RH, Clark CR, Gordon E. Cognitive aging, executive function, and fractional anisotropy: A diffusion tensor MR imaging study. Am J Neuroradiol 2007;28(2):226–235. [PubMed: 17296985]

Gunning-Dixon FM, Raz N. The cognitive correlates of white matter abnormalities in normal aging: A quantitative review. Neuropsychology 2000;14(2):224–232. [PubMed: 10791862]

Head D, Buckner RL, Shimony JS, Williams LE, Akbudak E, Conturo TE, et al. Differential vulnerability of anterior white matter in nondemented aging with minimal acceleration in dementia of the Alzheimer type: Evidence from diffusion tensor imaging. Cereb Cortex 2004;14(4):410–423. [PubMed: 15028645]

Henskens LH, Kroon AA, van Oostenbrugge RJ, Gronenschild EH, Hofman PA, Lodder J, et al. Associations of ambulatory blood pressure levels with white matter hyperintensity volumes in hypertensive patients. J Hypertens 2009;27(7):1446–52. [PubMed: 19502993]

Hofer S, Frahm J. Topography of the human corpus callosum revisited--comprehensive fiber tractography using diffusion tensor magnetic resonance imaging. Neuroimage 2006;32(3):989–994. [PubMed: 16854598]

Huang H, Zhang J, Jiang H, Wakana S, Poetscher L, Miller MI, et al. DTI tractography based parcellation of white matter: Application to the mid-sagittal morphology of corpus callosum. Neuroimage 2005;26 (1):195–205. [PubMed: 15862219]

Huang L, Ling XY, Liu SR. Diffusion tensor imaging on white matter in normal adults and elderly patients with hypertension. Chin Med J (Engl) 2006;119(15):1304–1307. [PubMed: 16919191]

Hugenschmidt CE, Peiffer AM, Kraft RA, Casanova R, Deibler AR, Burdette JH, et al. Relating imaging indices of white matter integrity and volume in healthy older adults. Cereb Cortex 2008;18(2):433–442. [PubMed: 17575289]

Kemper, T. Neuroanatomical and neuropathological changes during aging and dementia. In: Albert, ML.; Knoefel, J., editors. Clinical Neurology of Aging. Oxford University Press; New York: 1994. p. 3-67.

Kennedy KM, Raz N. Aging white matter and cognition: Differential effects of regional variations in diffusion properties on memory, executive functions, and speed. Neuropsychologia 2009a;47(3): 916–927. [PubMed: 19166865]

Kennedy KM, Raz N. Pattern of normal age-related regional differences in white matter microstructure is modified by vascular risk. Brain Res. 2009b in press.

Kochunov P, Thompson PM, Lancaster JL, Bartzokis G, Smith S, Coyle T, et al. Relationship between white matter fractional anisotropy and other indices of cerebral health in normal aging: Tract-based spatial statistics study of aging. Neuroimage 2007;35(2):478–487. [PubMed: 17292629]

Lenroot RK, Giedd JN. Brain development in children and adolescents: Insights from anatomical magnetic resonance imaging. Neurosci Biobehav Rev 2006;30(6):718–729. [PubMed: 16887188]

Madden DJ, Bennett IJ, Song AW. Cerebral White Matter Integrity and Cognitive Aging: Contributions from Diffusion Tensor Imaging. Neuropsychol Rev. 2009 Aug 25; 2009. Epub ahead of print.

Madden DJ, Spaniol J, Whiting WL, Bucur B, Provenzale JM, Cabeza R, et al. Adult age differences in the functional neuroanatomy of visual attention: A combined fMRI and DTI study. Neurobiol Aging 2007;28(3):459–476. [PubMed: 16500004]

Nyúl LG, Udupa JK. On standardizing the MR image intensity scale. Magn Reson Med 1999;42(6):1072–1081. [PubMed: 10571928]

O'Sullivan M, Summers PE, Jones DK, Jarosz JM, Williams SC, Markus HS. Normal-appearing white matter in ischemic leukoaraiosis: A diffusion tensor MRI study. Neurology 2001;57(12):2307–2310. [PubMed: 11756617]

Ota M, Obata T, Akine Y, Ito H, Ikehira H, Asada T, et al. Age-related degeneration of corpus callosum measured with diffusion tensor imaging. Neuroimage 2006;31(4):1445–1452. [PubMed: 16563802]

Pantoni L, Garcia JH. Pathogenesis of leukoaraiosis: A review. Stroke 1997;28(3):652–659. [PubMed: 9056627]

Paus T. Growth of white matter in the adolescent brain: Myelin or axon? Brain Cogn. 2009 in press.

Pfefferbaum A, Adalsteinsson E, Sullivan EV. Frontal circuitry degradation marks healthy adult aging: Evidence from diffusion tensor imaging. Neuroimage 2005;26(3):891–899. [PubMed: 15955499]

Pfefferbaum A, Sullivan EV. Increased brain white matter diffusivity in normal adult aging: Relationship to anisotropy and partial voluming. Magn Reson Med 2003;49(5):953–961. [PubMed: 12704779]

Pfefferbaum A, Sullivan EV, Hedehus M, Lim KO, Adalsteinsson E, Moseley M. Age-related decline in brain white matter anisotropy measured with spatially corrected echo-planar diffusion tensor imaging. Magn Reson Med 2000;44(2):259–268. [PubMed: 10918325]

Raz, N. Aging of the brain and its impact on cognitive performance: Integration of structural and functional findings. In: Craik, FIM.; Salthouse, TA., editors. The handbook of aging and cognition. Lawrence Erlbaum Associates; Mahwah, NJ: 2000.

Raz, N. The aging brain observed in vivo: Differential changes and their modifiers. In: Cabeza, R.; Nyberg, L.; Park, DC., editors. Cognitive Neuroscience of Aging: Linking Cognitive and Cerebral Aging. Oxford University Press; New York: 2005. p. 17-55.

Raz N, Lindenberger U, Rodrigue KM, Kennedy KM, Head D, Williamson A, et al. Regional brain changes in aging healthy adults: General trends, individual differences and modifiers. Cereb Cortex 2005;15(11):1676–1689. [PubMed: 15703252]

Raz N, Rodrigue KM. Differential aging of the brain: Patterns, cognitive correlates and modifiers. Neurosci Biobehav Rev 2006;30(6):730–748. [PubMed: 16919333]

Raz N, Rodrigue KM, Acker JD. Hypertension and the brain: Vulnerability of the prefrontal regions and executive functions. Behav Neurosci 2003;117(6):1169–1180. [PubMed: 14674838]

Raz N, Rodrigue KM, Kennedy KM, Acker JD. Vascular health and longitudinal changes in brain and cognition in middle-aged and older adults. Neuropsychology 2007;21(2):149–157. [PubMed: 17402815]

Roebroeck A, Galuske R, Formisano E, Chiry O, Bratzke H, Ronen I, et al. High-resolution diffusion tensor imaging and tractography of the human optic chiasm at 9.4 T. Neuroimage 2008;39(1):157–168. [PubMed: 17936015]

Salat DH, Tuch DS, Greve DN, van der Kouwe AJ, Hevelone ND, Zaleta AK, et al. Age-related alterations in white matter microstructure measured by diffusion tensor imaging. Neurobiol Aging 2005;26(8):1215–1227. [PubMed: 15917106]

Salat DH, Tuch DS, Hevelone ND, Fischl B, Corkin S, Rosas HD, et al. Age-related changes in prefrontal white matter measured by diffusion tensor imaging. Ann N Y Acad Sci 2005;1064:37–49. [PubMed: 16394146]

Schiavone F, Charlton RA, Barrick TR, Morris RG, Markus HS. Imaging age-related cognitive decline: A comparison of diffusion tensor and magnetization transfer MRI. J Magn Reson Imaging 2009;29 (1):23–30. [PubMed: 19097099]

Shrout PE, Fleiss JL. Intraclass correlations: Uses in assessing rater reliability. Psychological Bulletin 1979;2:420–428. [PubMed: 18839484]

Skoog I. A review on blood pressure and ischaemic white matter lesions. Dement Geriatr Cogn Disord 1998;9:13–19. [PubMed: 9716239]

Sled JG, Zijdenbos AP, Evans AC. A nonparametric method for automatic correction of intensity nonuniformity in MRI data. IEEE Trans Med Imaging 1998;17(1):87–97. [PubMed: 9617910]

Smith SM. Fast robust automated brain extraction. Hum Brain Mapp 2002;17(3):143–155. [PubMed: 12391568]

Song SK, Sun SW, Ju WK, Lin SJ, Cross AH, Neufeld AH. Diffusion tensor imaging detects and differentiates axon and myelin degeneration in mouse optic nerve after retinal ischemia. Neuroimage 2003;20(3):1714–1722. [PubMed: 14642481]

Song SK, Yoshino J, Le TQ, Lin SJ, Sun SW, Cross AH, et al. Demyelination increases radial diffusivity in corpus callosum of mouse brain. Neuroimage 2005;26(1):132–140. [PubMed: 15862213]

Sullivan EV, Adalsteinsson E, Hedehus M, Ju C, Moseley M, Lim KO, et al. Equivalent disruption of regional white matter microstructure in ageing healthy men and women. Neuroreport 2001;12(1): 99–104. [PubMed: 11201100]

Sullivan EV, Pfefferbaum A. Diffusion tensor imaging and aging. Neurosci Biobehav Rev 2006;30(6): 749–761. [PubMed: 16887187]

Sullivan EV, Rohlfing T, Pfefferbaum A. Quantitative fiber tracking of lateral and interhemispheric white matter systems in normal aging: Relations to timed performance. Neurobiol Aging. 2008 in press.

Sun SW, Liang HF, Trinkaus K, Cross AH, Armstrong RC, Song SK. Noninvasive detection of cuprizone induced axonal damage and demyelination in the mouse corpus callosum. Magn Reson Med 2006;55 (2):302–308. [PubMed: 16408263]

Tullberg M, Fletcher E, DeCarli C, Mungas D, Reed BR, Harvey DJ, et al. White matter lesions impair frontal lobe function regardless of their location. Neurology 2004;63(2):246–253. [PubMed: 15277616]

Van Boxtel MPJ, Henskens LH, Kroon AA, Hofman PAM, Gronenschild EHBM, Jolles J, et al. Ambulatory blood pressure, asymptomatic cerebrovascular damage and cognitive function in essential hypertension. J Hum Hypertens 2006;20(1):5–13. [PubMed: 16163365]

Verdelho A, Madureira S, Ferro JM, Basile AM, Chabriat H, Erkinjuntti T, et al. Differential impact of cerebral white matter changes, diabetes, hypertension and stroke on cognitive performance among non-disabled elderly. The LADIS study. J Neurol Neurosurg Psychiatry 2007;78(12):1325–1330. [PubMed: 17470472]

Vernooij MW, de Groot M, van der Lugt A, Ikram MA, Krestin GP, Hofman A, et al. White matter atrophy and lesion formation explain the loss of structural integrity of white matter in aging. Neuroimage 2008;43(3):470–477. [PubMed: 18755279]

Vernooij MW, Ikram MA, Vrooman HA, Wielopolski PA, Krestin GP, Hofman A, et al. White matter microstructural integrity and cognitive function in a general elderly population. Arch Gen Psychiatry 2009;66(5):545–553. [PubMed: 19414714]

Weissman MM, Sholomskas D, Pottenger M, Prusoff BA, Locke BZ. Assessing depressive symptoms in five psychiatric populations: A validation study. Am J Epidemiol 1977;106(3):203–214. [PubMed: 900119]

Westin CF, Maier SE, Mamata H, Nabavi A, Jolesz FA, Kikinis R. Processing and visualization for diffusion tensor MRI. Med Image Anal 2002;6(2):93–108. [PubMed: 12044998]

Wheeler-Kingshott CA, Cercignani M. About “axial” and “radial” diffusivities. Magn Reson Med 2009;61(5):1255–1260. [PubMed: 19253405]

Williams EJ. The comparison of regression variables. Journal of the Royal Statistical Society 1959;21:396–399.B

Yoshita M, Fletcher E, Harvey D, Ortega M, Martinez O, Mungas DM, et al. Extent and distribution of white matter hyperintensities in normal aging, MCI, and AD. Neurology 2006;67(12):2192–2198. [PubMed: 17190943]

Zahr NM, Rohlfing T, Pfefferbaum A, Sullivan EV. Problem solving, working memory, and motor correlates of association and commissural fiber bundles in normal aging: a quantitative fiber tracking study. Neuroimage 2009;44(3):1050–1062. [PubMed: 18977450]

Zhang Y, Du AT, Hayasaka S, Jahng GH, Hlavin J, Zhan W, et al. Patterns of age-related water diffusion changes in human brain by concordance and discordance analysis. Neurobiol Aging. 2008 in press.

Zhang YT, Zhang CY, Zhang J, Li W. Age-related changes of normal adult brain structure: Analysed with diffusion tensor imaging. Chin Med J (Engl) 2005;118(13):1059–1065. [PubMed: 16098256]

Zijdenbos AP, Forghani R, Evans AC. Automatic “pipeline” analysis of 3-D MRI data for clinical trials: application to multiple sclerosis. IEEE Trans Med Imag vol 2002;21(10):1280–1291.

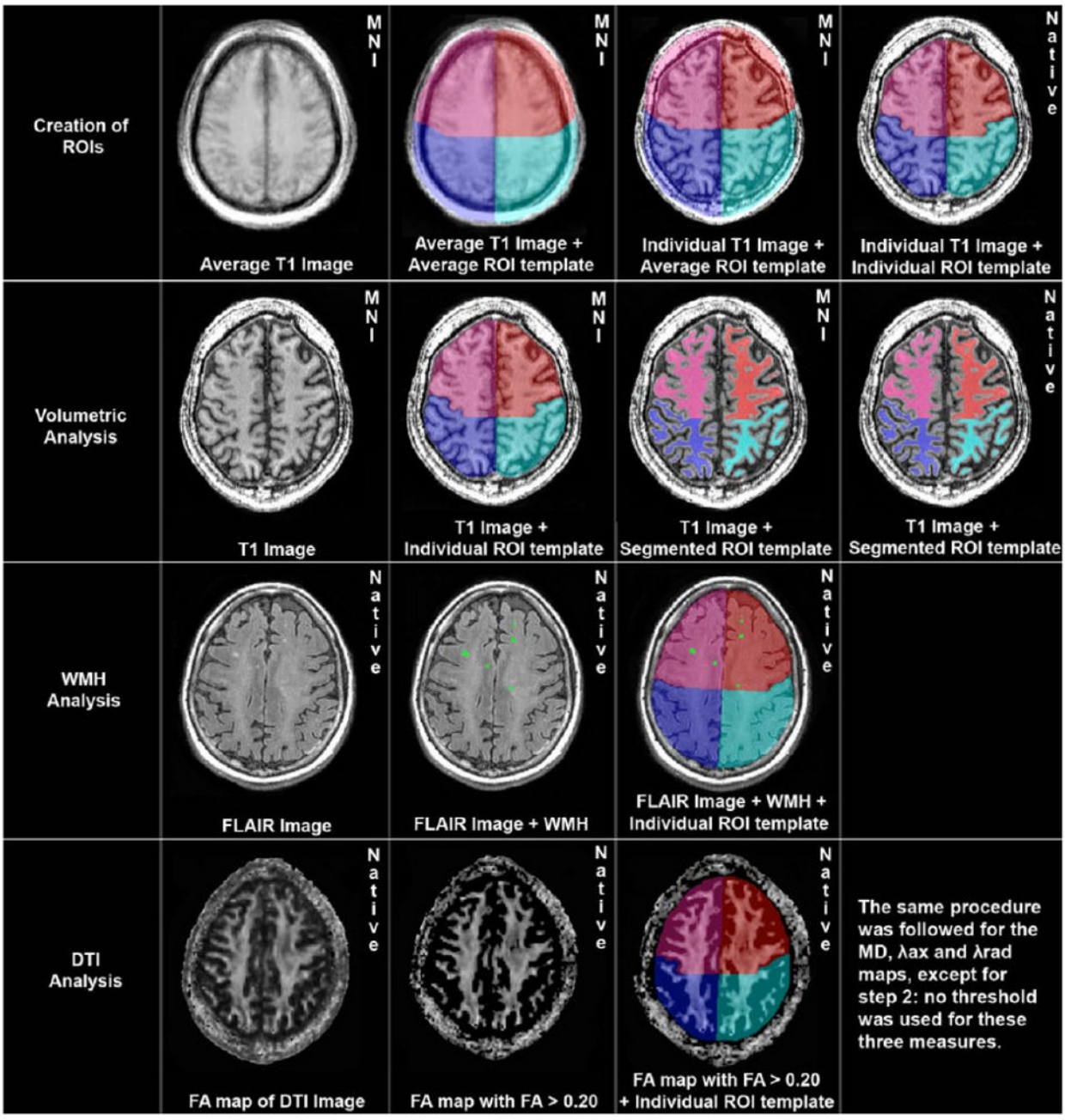

Figure 1.
Overview of the post-processing steps.

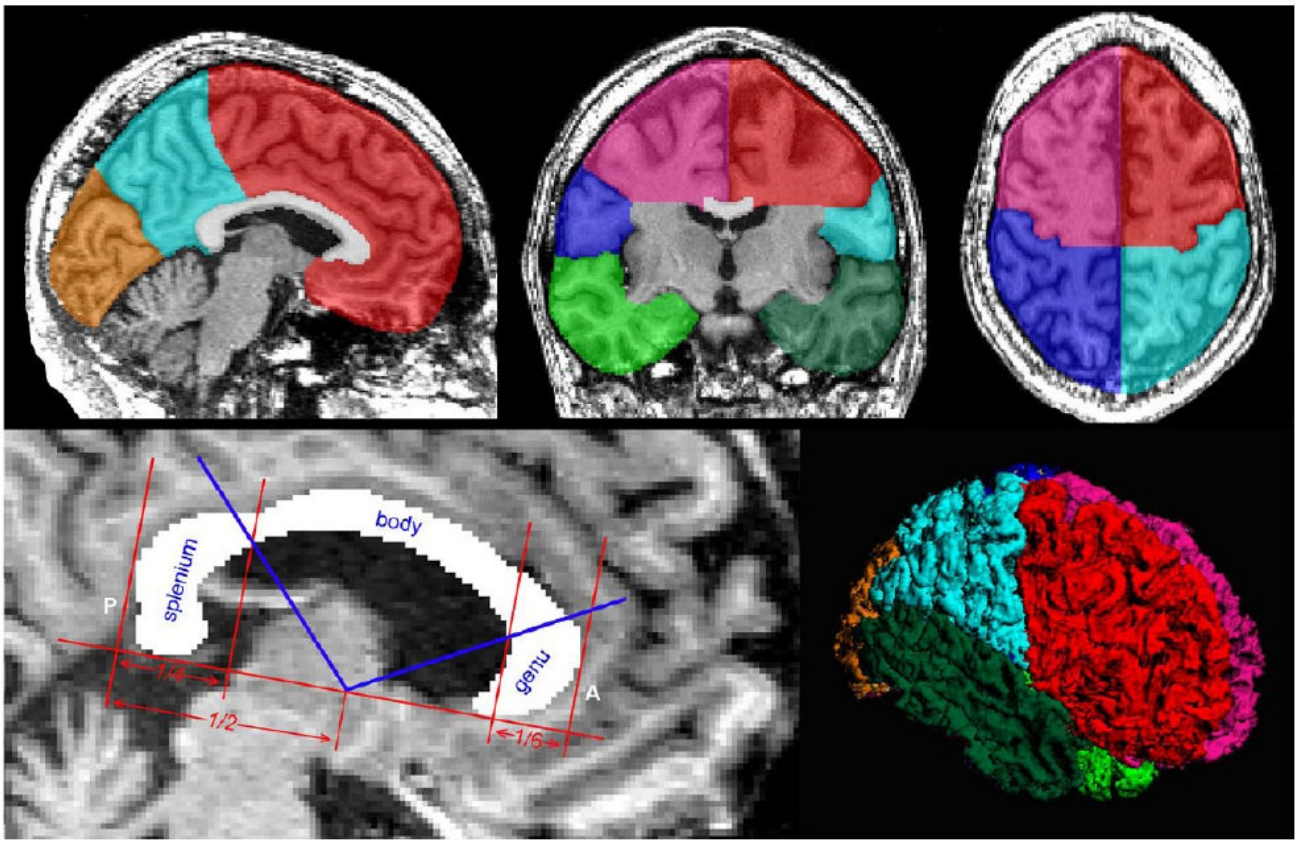

Figure 2.
Individual ROI template, indicating the regions of interest that were traced (corpus callosum: white; frontal lobe: red/pink; parietal lobe: dark/light blue; occipital lobe: orange; temporal lobe: dark/light green) and the subdivision of the corpus callosum (the blue lines divide the corpus callosum into genu, body and splenium)

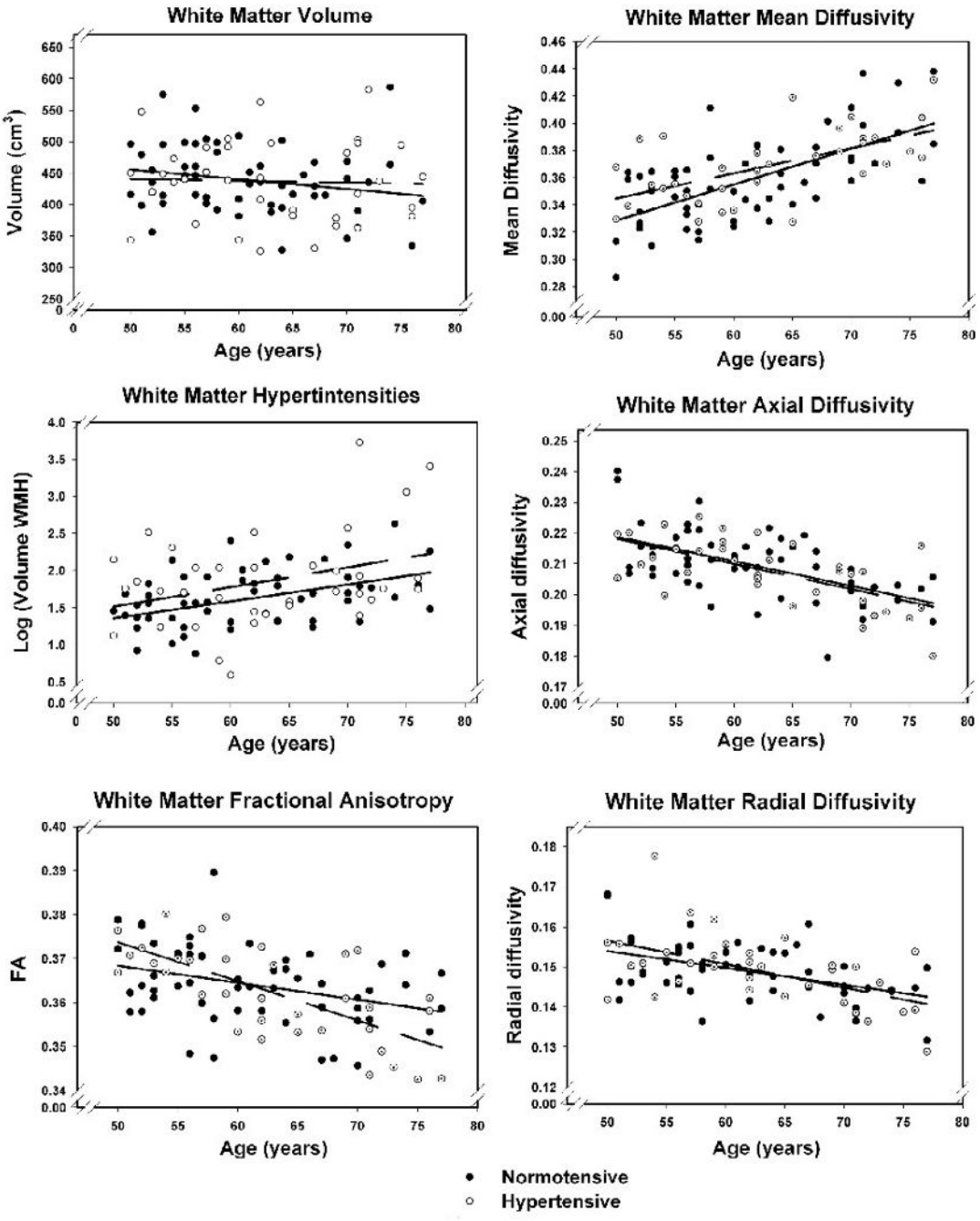

Figure 3.

Age differences in multiple indices of integrity of the total cerebral white matter. Note that Axial and Radial Diffusivity are relative indices (like functional anisotropy, FA), hence their association with age in the direction opposite to that of mean diffusivity.

Table 1

Description of the sample

	Men		Women		p-values of group comparisons; calculated by ANOVA (A) or χ^2 tests			
Variable; mean (SD) or %	**Normotensive**	**Hypertensive**	**Normotensive**	**Hypertensive**		**Sex**	**Hypertension**	**Sex×Hypertension**
Number of participants	25	15	32	21				
Age	61.4 (7.7)	61.1 (8.4)	61.2 (7.8)	64.7 (8.0)	A	0.438	0.253	0.279
Education in years	15.5 (2.6)	16.8 (3.3)	15.5 (2.6)	15.9 (2.4)	A	0.572	0.189	0.385
Caucasian race	68.0 %	80.0 %	75.0 %	52.4 %	χ^2	0.505	0.415	-
Hypertensive medication	0.0 %	86.7 %	0.0 %	85.7 %	χ^2	0.882	<**0.001****	-
Years of treatment with medication	0.0 (0.0)	6.1 (5.0)	0.0 (0.0)	5.5 (5.8)	A	0.900	<**0.001****	0.671
Systolic Pressure in mm Hg	122.7 (9.3)	133.6 (13.0)	120.8 (10.4)	134.6 (12.6)	A	0.844	<**0.001****	0.548
Diastolic Pressure in mm Hg	74.4 (5.4)	81.5 (9.4)	73.1 (6.4)	80.1 (4.9)	A	0.447	<**0.001****	0.972
MMSE	28.7 (1.2)	28.4 (1.1)	28.6 (1.0)	28.7 (0.7)	A	0.781	0.706	0.364
Intracranial volume in ml	1469.0 (147.2)	1435.8 (186.3)	1325.3 (111.3)	1259.7 (134.5)	A	<**0.001****	0.107	0.594

Note. Effects (of the continuous variables) were derived from the univariate ANOVA. Group differences (of the categorical variables) were evaluated by χ^2 tests.

** p<0.01.

Table 2

Table 2A. Effects of age and hypertension on white matter measures (white matter volume, WMH and FA)

		Effect of age		*Effect of hypertension*		*Age × hypertension interaction*		
	Mean (SD)	***F***	***p***	***F***	***p***	***F***	***P***	***ΔR²* in %**
Volume total	438.16 (58.75)	0.09	0.764	2.65	0.107	0.93	0.338	0.3
Volume CC genu	2.51 (0.42)	1.20	0.276	6.98	**0.010***	1.88	0.174	1.1
Volume CC body	4.38 (0.85)	5.82	**0.018***	0.38	0.538	3.45	0.067	2.9
Volume CC splenium	3.81 (0.66)	2.79	0.099	3.77	0.056	3.21	0.077	2.3
Volume FL	173.91 (24.77)	0.13	0.723	1.35	0.249	1.02	0.315	0.5
Volume PL	103.49 (14.69)	0.08	0.773	6.23	**0.015***	0.15	0.702	0.1
Volume OL	64.15 (9.73)	0.15	0.702	0.59	0.444	1.90	0.172	1.0
Volume TL	85.80 (14.74)	0.16	0.690	0.37	0.547	0.53	0.469	0.2
WMH total	5.52 (5.32)	7.65	**0.007****	0.04	0.837	0.22	0.644	0.2
WMH CC	0.00 (0.00)	-	-	-	-	-	-	-
WMH FL	0.85 (2.01)	3.37	0.070	0.90	0.345	1.47	0.229	1.4
WMH PL	0.47 (0.85)	0.00	0.981	6.15	**0.015***	6.85	**0.010***	6.7
WMH OL	2.97 (1.82)	5.55	**0.021***	0.31	0.582	0.17	0.686	0.1
WMH TL	0.78 (0.94)	2.70	0.104	2.91	0.091	4.00	**0.049***	3.5
FA total	0.363 (0.009)	7.49	**0.008****	4.25	**0.042***	4.53	**0.036***	3.7
FA CC genu	0.475 (0.082)	5.45	**0.022***	0.15	0.697	0.24	0.625	0.3
FA CC body	0.595 (0.032)	5.84	**0.018***	0.51	0.479	0.58	0.450	0.6
FA CC splenium	0.662 (0.035)	2.93	0.091	0.98	0.326	1.14	0.288	1.3
FA FL	0.354 (0.013)	6.60	**0.012***	13.16	<**0.001****	13.92	<**0.001****	9.4
FA PL	0.373 (0.012)	3.67	0.059	3.85	0.053	4.41	**0.039***	10.0
FA OL	0.348 (0.013)	6.38	**0.013***	0.00	0.995	0.04	0.849	0.1
FA TL	0.350 (0.009)	0.36	0.551	9.55	**0.003****	9.26	**0.003****	8.7

Table 2B. Effects of age and hypertension on additional DTI measures

		Effect of age		*Effect of hypertension*		*Age × hypertension interaction*		
	Mean (SD)	***F***	***p***	***F***	***p***	***F***	***P***	***ΔR²* in %**
		Effect of age		*Effect of hypertension*		*Age × hypertension interaction*		
	Mean (SD)	***F***	***p***	***F***	***p***	***F***	***p***	***ΔR²* in %**
MD total	0.362 (0.030)	52.78	<**0.001****	2.61	0.110	0.61	0.483	0.3
MD CC genu	0.312 (0.027)	17.19	<**0.001****	3.20	0.077	1.94	0.167	1.4
MD CC body	0.303 (0.030)	15.14	<**0.001****	0.58	0.448	0.13	0.715	0.1
MD CC splenium	0.282 (0.024)	11.98	**0.001****	0.09	0.769	0.05	0.829	0.1
MD FL	0.372 (0.029)	23.00	<**0.001****	0.30	0.587	0.37	0.542	0.3
MD PL	0.385 (0.038)	27.91	<**0.001****	0.15	0.697	0.00	0.975	0.0
MD OL	0.324 (0.029)	40.21	<**0.001****	0.40	0.531	0.00	0.999	0.0
MD TL	0.338 (0.025)	40.57	<**0.001****	3.58	0.062	0.65	0.424	0.4
AX total	0.209 (0.011)	28.79	<**0.001****	0.33	0.569	0.19	0.664	0.2
AX CC genu	0.376 (0.104)	5.39	**0.023***	0.24	0.627	0.16	0.690	0.1
AX CC body	0.547 (0.046)	3.29	0.073	0.45	0.504	0.08	0.780	0.1
AX CC splenium	0.636 (0.051)	1.58	0.212	0.73	0.396	3.20	0.077	3.6
AX FL	0.195 (0.014)	12.32	**0.001****	0.49	0.486	0.25	0.619	0.2
AX PL	0.195 (0.013)	11.81	**0.001****	0.12	0.734	1.57	0.214	1.3
AX OL	0.208 (0.014)	15.87	<**0.001****	0.21	0.652	0.44	0.507	0.4
AX TL	0.211 (0.011)	12.71	**0.001****	0.08	0.775	2.69	0.105	2.0
RAD total	0.149 (0.008)	13.09	<**0.001****	0.09	0.762	1.55	0.217	1.2
RAD CC genu	0.155 (0.015)	0.55	0.461	0.27	0.606	0.86	0.356	0.9
RAD CC body	0.135 (0.021)	3.23	0.076	0.14	0.712	2.34	0.129	2.6
RAD CC splenium	0.105 (0.029)	0.01	0.919	0.04	0.844	5.08	**0.027***	5.4
RAD FL	0.149 (0.010)	8.22	**0.005****	0.15	0.698	0.00	0.986	0.0
RAD PL	0.132 (0.010)	8.91	**0.004****	0.82	0.369	3.32	0.072	2.6

		Effect of age		*Effect of hypertension*		*Age × hypertension interaction*		
	Mean (SD)	***F***	***p***	***F***	***p***	***F***	***P***	***ΔR² in %***
RAD OL	0.155 (0.011)	10.65	**0.002****	0.05	0.830	0.31	0.580	0.2
RAD TL	0.168 (0.009)	8.44	**0.005****	1.10	0.298	3.15	0.080	2.6

Note. Effects of age and hypertension are from the multivariate General Linear Model (GLM). Volume = volume of white matter ROI in ml; WMH = volume of white matter hyperintensities in ml; FA = fractional anisotropy; CC = corpus callosum; FL = frontal lobe; PL = parietal lobe; OL = occipital lobe; TL = temporal lobe; F = F value; ΔR^2 = the incremental addition of explained variance after adding the interaction term to the model;

* p<0.05;

** p<0.01.

Note. Effects of age and hypertension are from the multivariate General Linear Model (GLM). MD = mean diffusivity; AX = relative axial diffusivity; RAD = relative radial diffusivity; CC = corpus callosum; FL = frontal lobe; PL = parietal lobe; OL = occipital lobe; TL = temporal lobe; F = F value; ΔR^2 = the incremental addition of explained variance after adding the interaction term to the model;

* p<0.05

** p<0.01.

Table 3

rrelation matrix for the four main indices of white matter integrity (volume, WMH, FA and MD)

	V_F	V_P	V_O	V_T	V_{genu}	V_{body}	V_{splen}	WMH_F	WMH_P	WMH_O	WMH_T	FA_F	FA_P	FA_O	FA_T	FA_{genu}	FA_{body}	FAs_{plen}	MD_F	MD_P	MD_O	MD_T	MD_{genu}	MD_{body}	MD_{splen}
4																									
1	.759																								
3	.782	.679																							
6	.831	.686	.848																						
2	.642	.691	.58	.617																					
0	.547	.611	.47	.477	.737																				
3	.624	.688	.54	.606	.792	.804																			
	.072	-.040	.11	.032	.115	-.106	.089																		
	.057	-.042	.15	.038	.017	-.121	-.027	.519																	
	.267	.193	.30	.393	.299	.008	.129	.413	.262																
	.129	.080	.17	.188	.201	-.030	.131	.653	.493	.646															
2	.164	.224	.08	.094	.136	.158	.193	-.245	-.307	-.122	-.246														
0	.165	.187	.11	.148	.118	.232	.226	-.286	-.391	-.138	-.242	.768													
0	.070	.076	.00	.035	.072	.190	.139	-.137	-.263	-.131	-.140	.672	.683												
7	.072	.092	-.00	-.080	.014	.043	.088	-.019	-.247	-.185	-.205	.701	.674	.719											
6	.244	.275	.17	.197	.310	.408	.380	-.057	-.101	-.024	-.116	.514	.302	.392	.342										
2	.139	.161	.13	.072	.216	.390	.239	-.122	-.060	-.022	-.137	.378	.333	.380	.315	.608									
4	-.023	.053	-.08	-.203	-.135	.035	-.028	.170	.015	-.138	-.055	.030	.197	.173	.208	-.004	.446								
	-.030	-.071	.051	.066	.010	-.209	-.227	.081	.174	.221	.328	-.313	-.235	-.347	-.321	-.422	-.262	-.100							
	-.053	-.084	.050	.101	-.008	-.278	-.227	.145	.216	.363	.362	-.334	-.217	-.263	-.263	-.451	-.325	-.092	.838						
	-.173	-.126	-.019	.001	-.074	-.295	-.238	.186	.217	.326	.338	-.410	-.258	-.358	-.289	-.512	-.474	-.168	.648	.831					
	.001	-.038	0.92	.137	.054	-.265	-.167	.223	.329	.423	.439	-.478	-.422	-.457	-.424	-.412	-.409	-.156	.714	.786	.822				
	-.142	-.212	-.066	-.060	-.216	-.413	-.272	.197	.275	.084	.222	-.465	-.418	-.352	-.272	-.438	-.397	-.082	.452	.489	.567	.630			
	.021	-.065	-.035	-.032	-.114	-.350	-.192	.128	.197	.201	.266	-.197	-.197	-.255	-.143	-.421	-.490	-.089	.453	.555	.589	.547	.643		
	-.158	-.273	-.099	-.170	-.203	-.304	-.368	.131	.120	.178	.218	-.445	-.357	-.352	-.302	-.563	-.415	-.125	.428	.508	.580	.503	.479	.594	

f white matter ROI; WMH = volume of white matter hyperintensities; FA = fractional anisotropy; MD = mean diffusivity; F = frontal lobe; P = parietal lobe; O = occipital lobe; T = temporal
f the corpus callosum; body = body of the corpus callosum; splen = splenium of the corpus callosum; |r| > 207 were significant at $p < 0.05$; |r| > .270 were significant at $p < 0.01$.